International Journal of Technical Research and Applications e-ISSN: 2320-8163,
www.ijtra.com Special Issue 28 (August, 2015), PP. 68-76

EVALUATION OF RUBBER COMPOUNDS FOR THE DEVELOPMENT OF WAVE ENERGY CONVERTER

Shamsul Kamaruddin[1], Alan E. Muhr[2], Grant E. Hearn[3]
[1]Engineering Design and Prototype Centre,
Malaysian Rubber Board
Sungai Buloh, Malaysia
[2]Engineering Design Unit,
Tun Abdul Razak Research Centre (TARRC)
Hertford, Herfordshire, United Kingdom
[3]Engineering and the Environment
University of Southampton
Southampton Boldrewood Innovation Campus
Burgess Road, Southampton, United Kingdom
[1]kshamsul@lgm.gov.my

***Abstract*— A wave energy converter (WEC) which is called Anaconda, is a cost effective wave energy device. The device seeks to exploit the concept of a distensible rubber tube. The concept of Anaconda has been proven at small laboratory scale and is seen as having low capital and operational costs. Different rubbers were quantified for building a good understanding of the range of stress-strain behavior and fatigue of rubber. The magnitude of the softening of several rubber formulations depends on the maximum strain applied. The larger the maximum strain applied, the greater the softening. A versatile tensile fatigue test machine was developed to enable a better understanding of fatigue, including non-relaxing fatigue to be developed for rubber or any other materials. For the fixed strain conditions used to screen candidate rubbers, a specific rubber compound performed the best compared both to the same unfilled rubber with antioxidant or no antioxidant in place, and a wide range of filled rubbers. The estimation on dynamic stress-strain loops and cyclic stress relaxation rates of each rubber has been made.**

Index terms— **wave energy converter (WEC), rubber, softening, stress-strain, modulus, loss angle, fatigue**

I. INTRODUCTION

Understanding the factors that affect the mechanical properties of rubber is essential for the development of a rubber based wave energy converter (WEC). A qualitative understanding of these factors is required in order to develop durable rubber compounds which can be used for the wave energy converter. The ability of rubber to withstand very large strains without failure or permanent deformation is the primary consideration making it attractive for playing a key role in a wave energy converter (e.g. Archimedes wave swing, Aquabuoy, Anaconda, Duck, Clam).

Wave energy extraction has recently become one of the priorities in the development of environmental friendly devices. A wave energy converter (WEC) which is called Anaconda, is a cost effective wave energy device [1]. The device seeks to exploit the concept of a distensible rubber tube. The concept of Anaconda has been proven at small laboratory scale and is seen as having low capital and operational costs. It was estimated that about 200 tonne of rubber will be used to manufacture the actual scale of Anaconda [2].

Several potential factors such as stress-strain behaviour, and fatigue life of rubber have been addressed together with an extensive experimental programme to provide some insight regarding advantageous rubber compounds appropriate to the development of rubber based devices offshore. The softening effect of a few large strain cycles on rubber is well known, However, there is little reporting of investigations based on a very large number of strain cycles with the unusual feature of incomplete relaxation. In this research, these are a large number of cycles at strains much greater than previously investigated. Apart from the data of Cadwell et al. (1940) [3] and the Engineering Data Sheets (EDS) (Natural Rubber EDS 1979) [4] there is no comprehensive data on fatigue properties of natural rubber under strain cycle levels relevant to arduous non-relaxing cycles. Only the data of Cadwell et al. (1940) extends to the full life time; in the EDS, fatigue tests were aborted at 2Mcycles. As well as being limited to a single material, the data of Cadwell et al. (1940) gives no information on the range or standard deviation of the replicate tests, as would be required in any estimation of the number of expected failings over a preferred operational period of any rubber component. The objectives of this research work were to quantify and build a good understanding of the range of stress-strain behaviour exhibited by different rubbers and also

Ingredients	A1	A2	A3	A4	A5	A6	A7
	pphr						
Natural rubber (NR), SMRCV60	100	100	100	100	100	100	100
Carbon black, HAF (ASTM N-330)	-	15	30	45	-	-	-
Carbon black, HAF (ASTM N-990)	-	-	-	-	30	37.5	45
process oil (410 Oil)	-	1.5	3.0	4.5	3	3.8	4.5
Zinc oxide	5	5	5	5	5.5	5.5	5.5
Stearic acid	2	2	2	2	1.5	1.5	1.5
Antioxidant 2246	-	3	3	3	-	-	-
Antioxidant HPPD	-	-	-	-	3	3	3
Antiozonant wax (Negazone)	-	2	2	2	-	-	-
Accelerator, CBS	0.6	0.6	0.6	0.6	0.8	0.8	0.8
Sulfur	2.5	2.5	2.5	2.5	2.9	2.9	2.9
Cure Condition (Time,min Temperature, °C)	45, 140	38, 140	40, 140	40, 140	30, 140	30, 140	30, 140

to provide further insight and experimental capability into fatigue of rubber.

II. MATERIALS and test procedures

The sheets of investigated compounds of Tables I had a nominal thickness of 2mm and were moulded according to the cure conditions specified in each table. Most of the compounds were cured as nominal 2mm thick sheets. The cure characteristics of the mixed compounds were determined by an oscillatory disc rheometer (Mosanto Rheometer MDR2000). The test pieces were cut from the appropriate sheet and the dimensions of each test piece (following sample ID) are provided in Table II.

Three hardness buttons of each compound were cured and used for hardness tests in accordance with the standard BS ISO 48:2007; results are provided in Table II.

Three tensile dumb-bells (Type 2, BS ISO 37:2005) were cut from cured sheet from each compound. Tensile strength tests were conducted using an Instron 5567 machine equipped with an extensometer. The crosshead speed was 500mm/min, a load cell of 500N was used and all the data recorded using an Instron BlueHill software program. A gauge length on the narrow part of the dumbbell test piece was marked using a ϕ6mm white sticker. The gauge length of the test piece was approximately 20mm in the extensometer viewfinder, which has a range of 500mm in height and 50mm in width. The initial distance between the two grips was 50mm. All the tests were carried out according to BS ISO 37:2005 [5].

TABLE I. Formulations of the rubber compounds mixed

TABLE II. Dimension of each tensile strip and the hardness test results.

Sample ID	Dimension (mm)	Hardness, (IRHD)
A1	1.92 x 5.92 x 160	41
A2	2.01 x 5.92 x 160	49
A3	1.92 x 5.95 x 160	57
A4	1.95 x 5.91 x 160	66
A5	1.90 x 5.85 x 160	53
A6	2.06 x 5.86 x 160	36
A7	1.93 x 5.82 x 160	57

The room temperature stress-strain cyclic tests were conducted, on parallel sided tensile strips (as specified in Table II) using an Instron 4701 universal test machine. The length of each sample between clamps was 150mm.

Each testpiece was stretched to 50%, 100%, 150%, 200%, 250% and 300% of original length consecutively for 3 cycles at each strain and at a strain rate of $0.0167s^{-1}$, returning to the original clamp separation between each stretch. Next each sample was tested one half cycle to 160% followed by three cycles, starting from 160%, with a sequence of strain amplitudes of 15%, 25%, 35%, 45%, 55%, 95% and 105%. These strain cycles were chosen to represent possible excitation during the impingement of waves on the application device, in addition to its design static strain of 160%. The cycle 160±105% represents the maximum excitation.

A personal computer with Picologger was used to record all the force and displacement data. The data acquisition sampling rate was 1.5Hz, so that a load-deflection data point was captured for every 3s approximately. The load-cell used in the tests typically had a range of ±1kN. The load-cell was changed to 100N when uniaxial tension tests were conducted on rubber compounds with a hardness below 50IRHD, to obtain more accurate results.

Stress and strain data were calculated based on the dimensions of each test piece using Microsoft Excel 2010.

Design for the application requires knowledge of the elastic modulus of the rubber. For a typical application, it may be sufficient to know the equivalent linear dynamic properties, stiffness and loss angle, for dynamic strain cycles applied to the component in its static state of strain. In case of rubber in a strain state approximating to tension, these dynamic properties may readily found using the secant method [6], adapted to a cyclic tensile strain superimposed on a static tensile strain. The basic equations are given in Equations (1) and (2), with the symbols defined in the hysteresis loop shown in Figure 1. The loss angle provides a measure of the damping or hysteresis energy losses within rubber subjected to cyclic deformation. The modulus and loss angle were determined by applying the secant method illustrated in Figure 1:

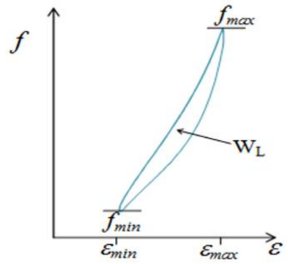

Fig. 1. Hysteresis loop showing non-linear behaviour typical of filled rubber at high strain [6].

$$\delta = \frac{4W_L}{(\varepsilon_{max} - \varepsilon_{min})(f_{max} - f_{\min})} \tag{1}$$

$$|E^*| = \frac{f_{max} - f_{min}}{(\varepsilon_{max} - \varepsilon_{min})} \tag{2}$$

Note that this equivalent linearisation does not distinguish between kinematic and material origin of nonlinear stress-strain behaviour. In Equation (2) the strain is calculated with respect to the reference length of the test piece. If instead the dynamic strain amplitude were calculated with respect to the prestrained state, the dynamic strain would be reduced according to

$$e = \frac{\Delta x}{(1+\varepsilon_0).x_0} = \frac{1}{1+\varepsilon_0}.\frac{\Delta x}{x_0} = \frac{1}{1+\varepsilon_0}.\varepsilon \tag{3}$$

where ε_0 is the static prestrain, equal to 1.6 here.

A visual basic program was created to calculate the modulus and loss angle using Equations (2) to (3). All the experimental data sets were partitioned into a number of distinct cycles using Excel. The program then enabled the calculation of the modulus and loss angle by specifying the columns of time, displacement and force, as well as the number of the cycle.

A versatile tensile fatigue test machine was developed. It is enable a better understanding of fatigue, including non-relaxing fatigue to be developed for rubber or any other materials. Figure 2 shows the fatigue machine which has 6-station located at the top and bottom rows respectively.

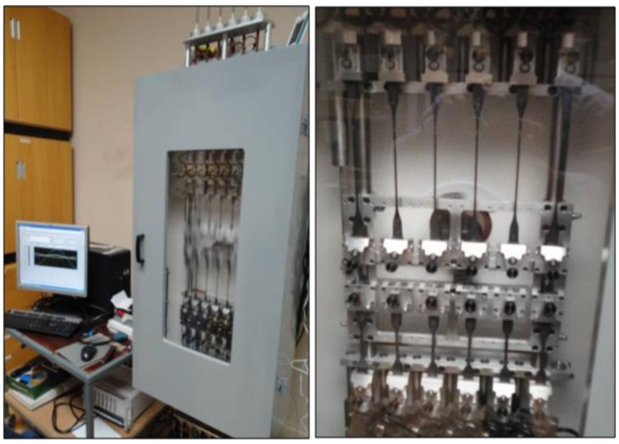

Fig. 2. Twelve station fatigue test machine

In these tests, the rubber formulations as mentioned in Table I were used. Twelve tensile dumbbells Type 2 (BS ISO 37:2005) were cut from 7 different cured sheets. Two gauge lines were introduced with a separation of 22mm in the middle of each test piece. The desired frequency of the fatigue tests is not attained instantaneously. Typically the first 150 cycles may be considered transient in recording behaviour from test initialization to attainment of require oscillation frequency. There are 12 dedicated load cells monitoring the loading of the 12 samples. A Labview-based system records all the data for each load cell. It also logs the LVDT transducer giving the carriage position as a function of time. We can define a stable user interrogation frequency once the first 150 cycles have been completed. In these experiments the interrogation frequency for generating output record is 1000 cycles at a frequency of 4.49Hz until sample failure occurs in all 12 test pieces. All materials were subjected to non-relaxing strain cycles with a minimum strain of 55% (34.1mm displacement) and maximum strain of 265% (80.3mm displacement). Figure 1 shows the upper six samples set at the maximum strain and the lower six samples experiencing the minimum strain. As the upper samples attain maximum strain so the lower samples undergo the minimum strain and increasing to maximum strain.

The separation of the indicated gauge lines were measured accurately using a vernier calliper. The fatigue lives of all rubbers in the non-relaxing tests were compared. Ozone concentration in the test chamber was measured using UV Photometric Ozone Analyzer-Model 1008. The average ozone concentration in the test chamber was 0.003ppm. The temperature and humidity in the test chamber were also measured using a digital combination of thermometer, hygrometer and clock (TEMPTEC Indoor and Outdoor Temp: Thermo-Hygrometer-Clock). The average temperature and humidity were 20°C and 752%, respectively.

III. RESULTS AND DISCUSSION

A. Stress-strain behavior under cyclic states

Table III shows the overall results of rubber compounds for modulus, tensile strength and elongation at break. Different fillers give different properties of modulus, tensile strength and elongation at break. The higher the content of filler, the greater the modulus and decrease the elongation at break. In contrast, the elongation at break decreases as the filler content is increased. The tensile strength is not significantly affected by filler content.

TABLE III. OVERALL RESULTS OF MODULUS, TENSILE STRENGTH AT ELONGATION AT BREAK FOR ALL COMPOUNDS.

Sample ID	Median Modulus (100%), (MPa)	Median Tensile Strength (MPa)	Median Elongation at Break (%)
A1	0.79	26.67	693
A2	1.09	29.54	725
A3	1.83	31.47	621
A4	2.49	28.47	557
A5	1.44	25.80	587
A6	1.55	25.91	647
A7	1.67	24.09	590

When the content of carbon black is increased so the modulus, hysteresis and stress-softening also increase. Most softening occurs during the first deformation, and after a few stress cycles a steady state is approached. Figure 3 illustrates the displacement–time plot of one of the tensile stress-strain cyclic tests. Figure 4 shows the plot of all data point of displacement and force in non-relaxing for one of the tensile stress-strain cyclic tests.

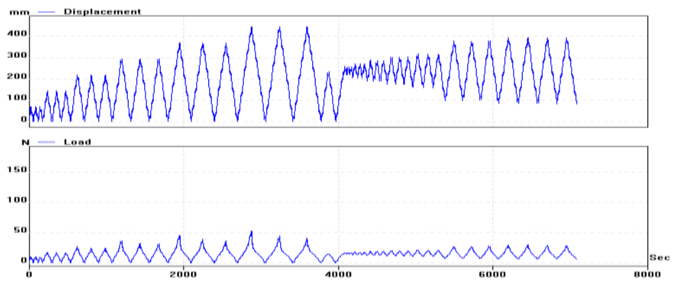

Fig. 3. Example of displacement-time plot of cyclic test for A6 compound.

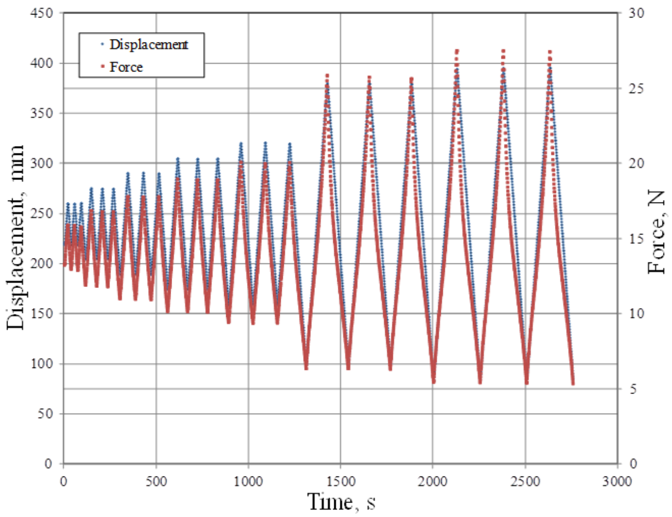

Fig. 4. Example of the data point plot of displacement in non-relaxing for compound displacement-time plot of cyclic test for A6 compound.

Figures 5 – 18 provide relaxed and non-relaxed stress strain curves for materials of Table I. A1 is unfilled, and hence Figures 5 and 6 reveal the desirable characteristics of very low set, hysteresis and stress-softening, but the material is rather soft. Other materials reported in Figures 7 to 11 are reinforced and exhibit more hysteresis and stress-softening. This might be worth tolerating in return for the higher stiffness.

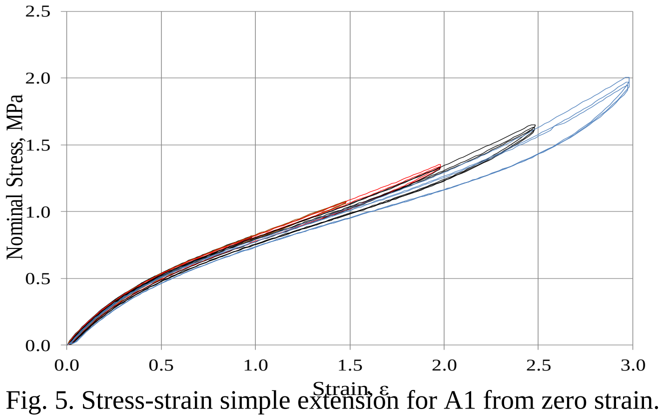

Fig. 5. Stress-strain simple extension for A1 from zero strain.

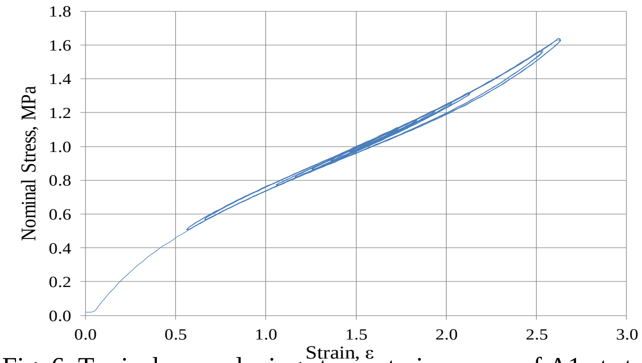

Fig. 6. Typical non-relaxing stress-strain curves of A1 at strain amplitude of 15%, 25%, 35%, 45%, 55%, 95% and 105%.

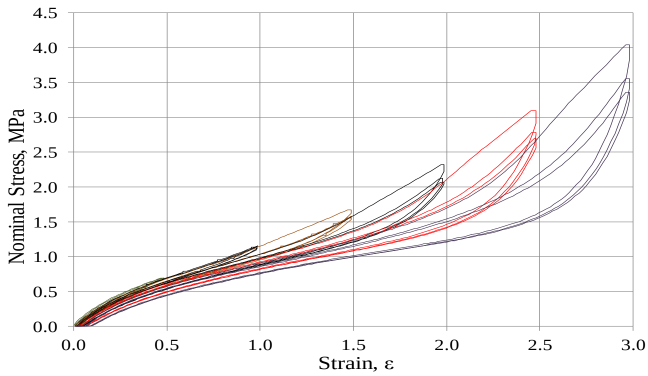

Fig. 7. Stress-strain in simple extension for A2 from zero strain.

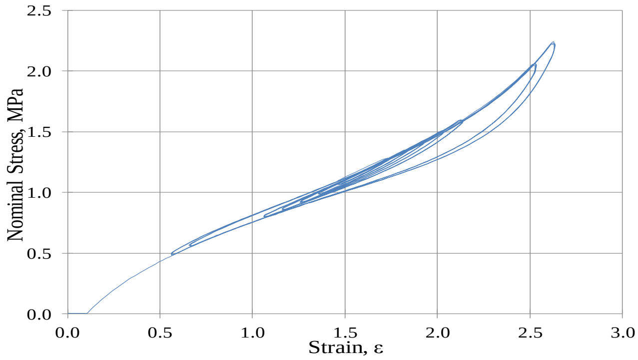

Fig. 8. Typical non-relaxing stress-strain of A2 at strain amplitude of 15%, 25%, 35%, 45%, 55%, 95% and 105%.

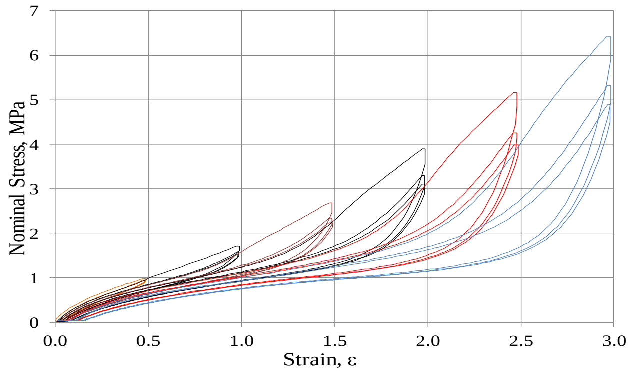

Fig. 9. Stress-strain in simple extension for A3 from zero strain.

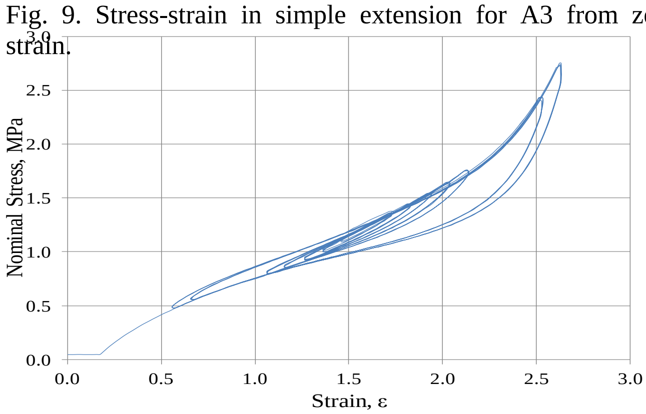

Fig. 10. Typical non-relaxing stress-strain of A3 at strain amplitude of 15%, 25%, 35%, 45%, 55%, 95% and 105%.

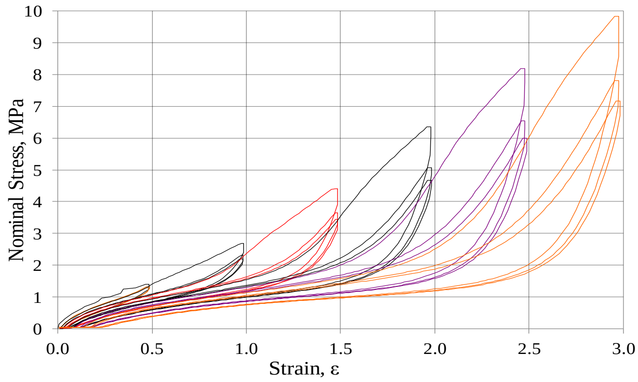

Fig. 11. Stress-strain in simple extension for A4 from zero strain.

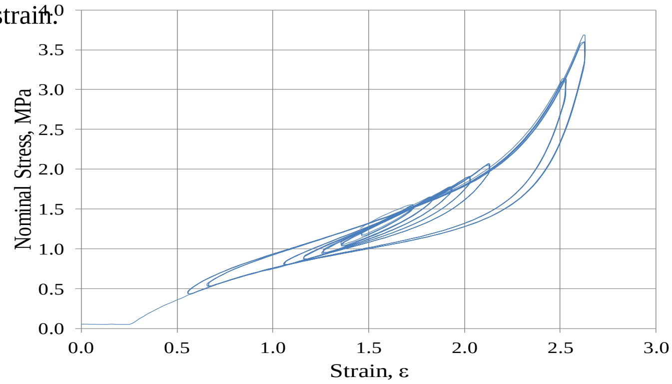

Fig. 12. Typical non-relaxing stress-strain of A4 at strain amplitude of 15%, 25%, 35%, 45%, 55%, 95% and 105%.

.

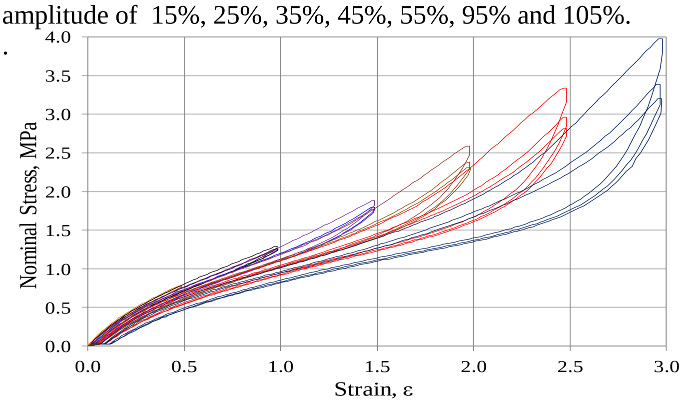

Fig. 13. Stress-strain in simple extension for A5 from zero strain.

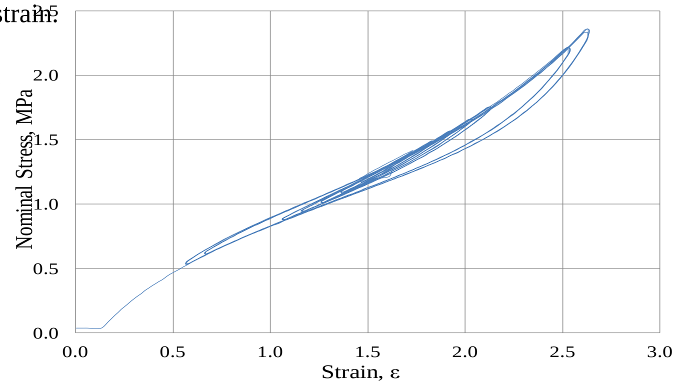

Fig. 14. Typical non-relaxing stress-strain of A5 at strain amplitude of 15%, 25%, 35%, 45%, 55%, 95% and 105%.

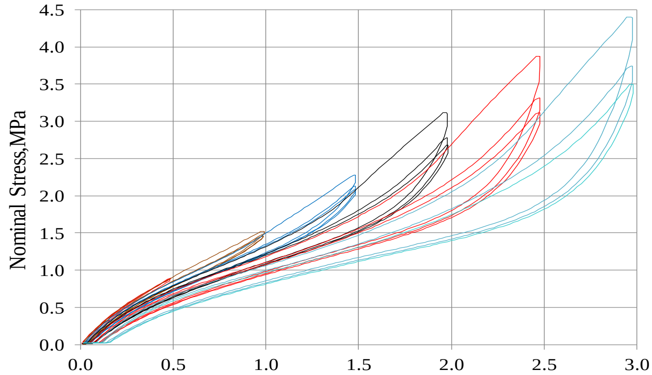

Fig. 15. Stress-strain in simple extension for A6 from zero strain.

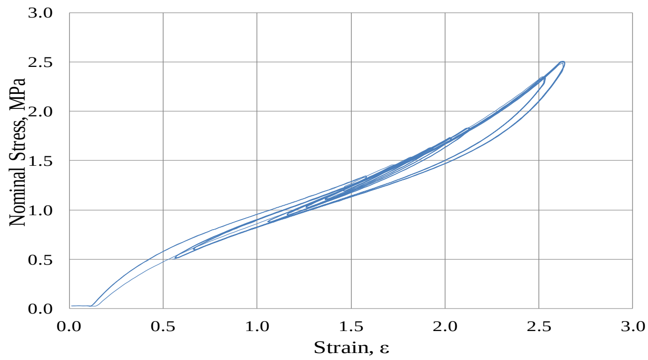

Fig. 16. Typical non-relaxing stress-strain of A6 at strain amplitude of 15%, 25%, 35%, 45%, 55%, 95% and 105%.

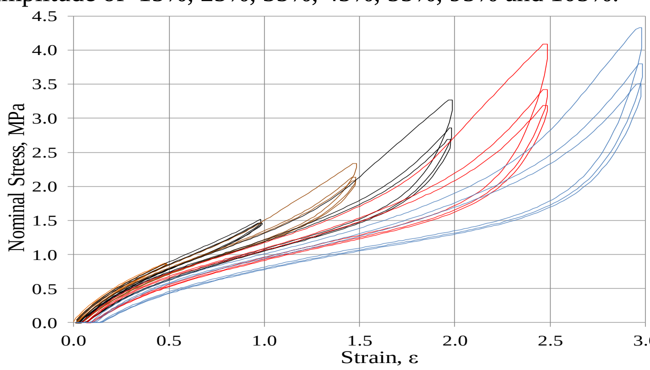

Fig. 17. Stress-strain in simple extension for A7 from zero strain.

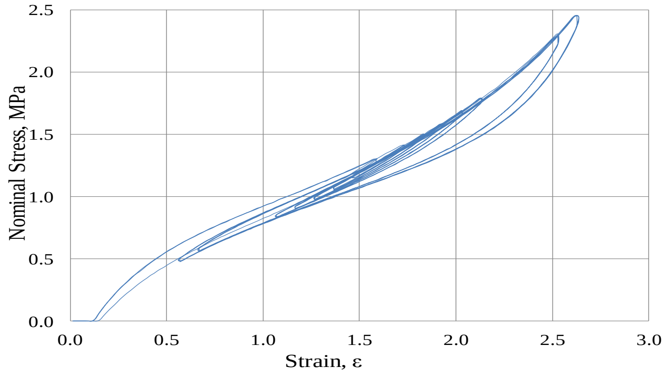

Fig. 18. Typical non-relaxing stress-strain of A7 at strain amplitude of 15%, 25%, 35%, 45%, 55%, 95% and 105%.

The presence of filler reduces the fatigue for the given conditions, in the coarse non-reinforcing types like N990 used in the A5 ~ 7 materials -having a particularly adverse effect, in a similar way to the EDS series using N330 black. It is confirmed that the rubbers with reinforcing filler have shown a higher set, hysteresis and stress for a given strain. Thus key aspects of material formulations can be predicted by comparing their stress-strain behaviour including the modulus, tensile strength, elongation at break and hardness.

All the rubber compounds showed stress softening at large strain, but the magnitude of the effect increased strongly with increase in filler content. The stress-strain curves were nearly stabilized after 3 cycles although the stress slightly diminishes with further cycles.

It is found that for unfilled natural rubber at low strain, there is little hysteresis, but it is very much greater at high strain. It is believed that the large hysteresis for unfilled natural rubber at high strains is due to crystallization.

The large initial hysteresis for the filled compound is believed to be associated with rearrangement of loading paths or bonds in the elastomer filler material system [7]. After cyclic uniaxial tension tests, rubbers show a permanent set in the direction of stretching.

All the non-relaxing stress-strain cycles were carried out immediately after completing the fully relaxing stress-strain tests. There was little further stress-softening in the non-relaxing tests. The rubber compound of A1 showed less effect of stress softening in non-relaxing cyclic excitation.

Generally, the difference between the various tested materials was less striking for the non-relaxing cycles. It is possible partly because they are in the “scragged” or “post-Mullins” state [8]. Low hysteresis in non-relaxing stress-strain cycles is often desirable, for example for a rubber device designed to store energy.

Figure 19 shows stress-strain curves of each strain amplitude for A4 where the centre position of each hysteresis loop is at a strain of 1.5.

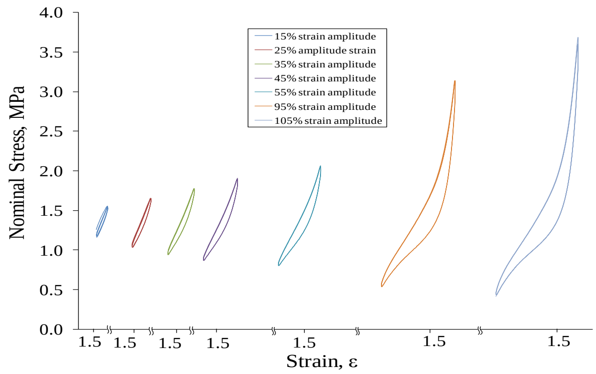

Fig. 19. Separation of stress-strain curves for each strain amplitude A4.

Tables IV and V show the resulting values of modulus and loss angle for each rubber compound.

Modulus and loss angle were calculated from the average of the results obtained for each of the three consecutive full non-relaxing cycles starting from the given minimum strain.

TABLE IV. Results of dynamic modulus and loss angle for A1~A4 rubber compounds.

	A1		A2		A3		A4	
Amplitude, %	Loss angle (degrees)	Modulus (secant) (MPa)	Loss angle (degrees)	Modulus (secant) (MPa)	Loss angle (degrees)	Modulus (secant) (MPa)	Loss angle (degrees)	Modulus (secant) (MPa)
15	6.88	0.50	8.55	0.78	12.33	0.98	15.29	1.34
25	3.92	0.49	5.91	0.75	9.06	0.93	11.36	1.24
35	3.18	0.50	5.23	0.75	8.30	0.91	10.77	1.22
45	2.72	0.51	5.08	0.74	8.27	0.88	10.82	1.18
55	2.57	0.51	5.37	0.74	8.78	0.87	9.81	1.13
95	2.14	0.52	4.74	0.77	7.42	0.94	9.34	1.38
105	2.40	0.55	5.26	0.83	7.85	1.06	8.58	1.55

TABLE V. RESULTS OF DYNAMIC MODULUS AND LOSS ANGLE FOR A5~A7 RUBBER COMPOUNDS.

	A5		A6		A7	
Amplitude, %	Loss angle (degrees)	Modulus (secant) (MPa)	Loss angle (degrees)	Modulus (secant) (MPa)	Loss angle (degrees)	Modulus (secant) (MPa)
15	7.70	0.86	8.39	0.94	8.98	0.93
25	5.00	0.86	5.36	0.92	5.81	0.94
35	4.43	0.82	4.67	0.90	5.13	0.90
45	4.06	0.81	4.36	0.91	4.96	0.90
55	3.61	0.82	3.86	0.88	4.45	0.87
95	4.73	0.86	4.95	0.94	5.88	0.93
105	4.87	0.88	5.03	0.96	5.96	0.95

The addition of filler caused a large increase in magnitude of the modulus and hysteresis. The modulus of filled rubber is approximately constant except for a small increase at the highest amplitudes whereas the modulus of unfilled rubber is little affected by strain amplitude.

Filled vulcanizates give higher loss angles, with the value depending upon the type and amount of filler. The higher angles are associated with breakdown of the interactions responsible for the high stiffness at low strains [9].

B. Non-relaxing fatigue analysis

Tables VI shows the results of fatigue tests in a non-relaxing state condition for all rubbers. The comparison with other rubbers was made based on the average of the number of cycles to failure. The numbers of cycles to failure of the author modified EDS19 recipe, A1 was much better than others. It is confirmed that carbon blacks contained in author modified rubber A2 has minimised the fatigue life under these conditions of fixed strain.

TABLE VI. Dimension of each tensile strip and the hardness test results.

Sample	No. of cycle						
	A1	A2	A3	A4	A5	A6	A7
1-1	39,480	46,160	4,240	7,110	54,130	34,720	26,670
1-2	46,120	48,050	11,520	6,220	75,600	16,550	17,110
1-3	108,140	49,890	7,490	2,000	64,210	50,910	45,760
1-4	71,420	39,380	7,120	5,140	59,170	36,160	45,020
1-5	49,210	35,110	10,220	4,620	67,970	16,270	20,300
1-6	90,820	40,080	9,560	4,960	66,230	68,400	41,210
2-1	173,570	35,700	13,080	4,720	80,290	43,340	44,570
2-2	108,590	40,020	15,010	1,920	25,950	5,040	25,030
2-3	99,300	44,630	9,440	5,460	82,710	51,700	7,820
2-4	40,640	37,800	14,330	4,850	22,900	7,400	34,900
2-5	62,050	35,010	12,580	4,030	92,910	5,550	11,420
2-6	115,860	35,540	13,600	4,890	83,790	71,500	20,450
Average	**83,767**	**40,611**	**10,683**	**4,660**	**64,655**	**33,962**	**28,355**
Standard Deviation	**40,060**	**5,308**	**3,275**	**1,492**	**21,848**	**23,848**	**13,578**
Median	**81,120**	**39,690**	**10,870**	**4,870**	**67,100**	**35,440**	**25,850**

Figures 20~23 show the relationship of fatigue life and all properties stated in Table III. Figure 20 shows the overall results of fatigue test for all rubber compounds by ranking based on the number of cycles to failure. The hardness value of each compound was measured and a weak inverse correlation with fatigue test results is evident in Fig. 20.

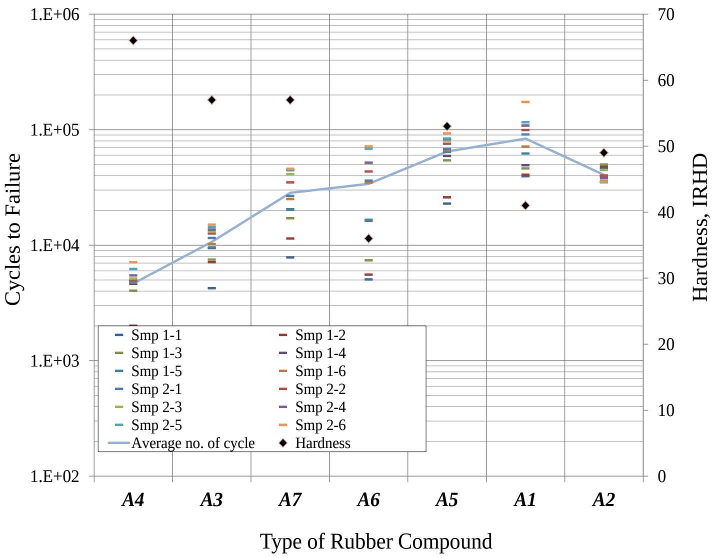

Fig. 20. Overall fatigue test results of all rubber compounds at 160±105% strain. The relationship of fatigue test results and hardness was plotted for comparison.

Figure 21 presents fatigue test data with tensile strength data for each compound. It is apparent that the tensile strength is not correlated with fatigue life.

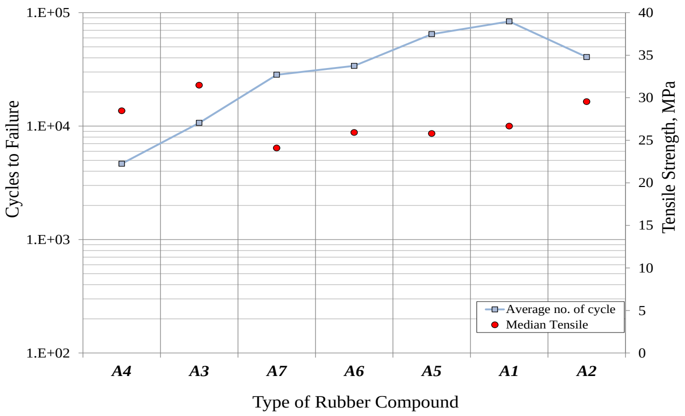

Fig. 21. Overall fatigue test results of all rubber compounds at 160±105% strain. The relationship of fatigue test results and tensile strength was plotted for comparison.

Figure 22 addresses elongation at break and fatigue test data for rubber compounds examined. It is apparent that high elongation at break correlates fairly well with fatigue life.

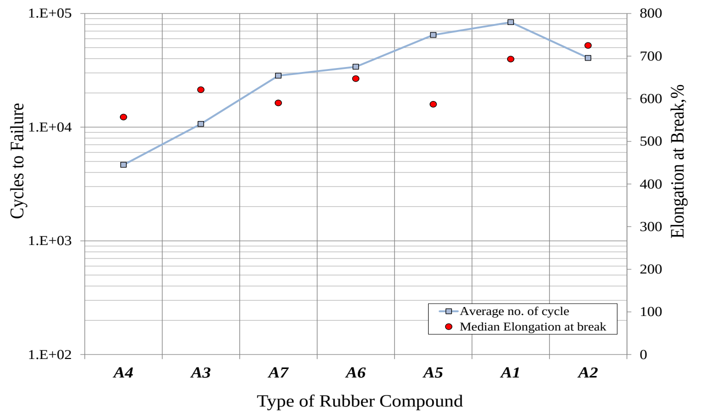

Fig. 22. Overall fatigue test results of all rubber compounds at 160±105% strain. The relationship of fatigue test results and elongation at break was plotted for comparison.

Figure 23 shows that the mean fatigue life of the rubber compounds correlates inversely with that modulus (100%).

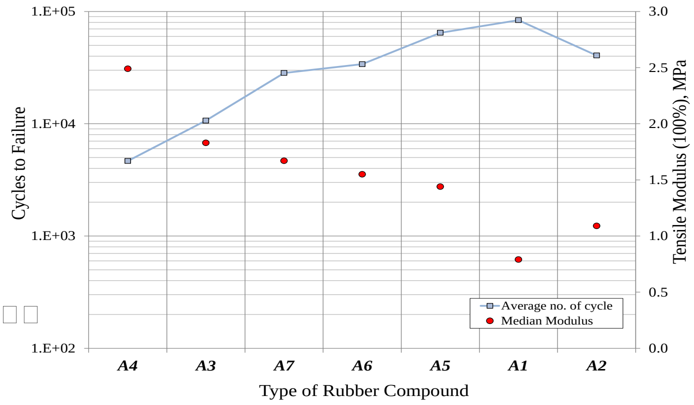

Fig. 23. Overall fatigue test results of all rubber compounds at 160±105% strain. The relationship of fatigue test results and tensile modulus was plotted for comparison.

IV. CONCLUSIONS

The magnitude of the softening depends on the maximum strain applied. The larger the maximum strain applied, the greater the softening. This is known as the Mullins effect. The higher the carbon black loading, the greater the stress-softening and hysteresis.

Hysteresis of the unfilled rubbers does become large at very high amplitudes, probably indicating strain-crystallisation.

A 12-station fatigue test machine integrated with a Labview data logging was successfully developed. This machine can be used to apply a wide range of strain amplitudes in either relaxing or non-relaxing conditions. For the fixed strain conditions (160±105%) used to screen candidate rubbers, A1 performed the best compared with a wide range of filled rubbers.

In these tests being constant strain, the modulus of the test rubber correlates inversely with fatigue life

Softening to cycling between fixed strain limits continues at an approximately constant rate per tenfold increase in number of cycles. The amount of carbon black content affects the softening behaviour of rubber. Lower amounts of carbon black result in less hysteresis and a longer fatigue life for fixed strain cycles.

Modulus and loss angle of each rubber were determined in tension for samples prestrained to 160% for a range of dynamic amplitudes (15% to 105%). It was found that the loss angle decreased when the dynamic amplitude increased, and was surprisingly large (6.9^o for unfilled NR) at the smallest amplitude (15%). For filled NR, the Payne effect - i.e. fall in dynamic modulus as the strain amplitude is increase - was surprisingly weak. At the highest two strain amplitudes (95% and 105%) the modulus of the filled rubber increases, presumably because the maximum strain is very high (255% and 265% respectively) so that affects of strain crystallization and/or finite extensibility result in an upturn in the stress-strain curves.

Unfilled natural rubber is the most appropriate material that should be used since it has a long fatigue life for large strain amplitudes and non-relaxing conditions with low modulus. It is not a good idea to use a lot of filler in natural rubber because it will make the fatigue life of rubber shorter.

Acknowledgment

The authors wish to thank Malaysian Rubber Board for the permission to publish this research paper. Assistance given by Dr Julia Gough, Ian Stephen, Robert Picken, Judith Picken and Alan Harris at TARRC throughout this work is also highly appreciated.

References

[1] Farley, F.J.M. and Rainey, R.C.T., “Radical design options for wave-profiling wave energy converters”, 21st International Workshop on Water Waves and Floating Bodies, Loughborough, UK, 2006, pp 1-4

[2] Bucchi, A. and Hearn, G.E., “Delay or removal of aneurysm formation in the Anaconda wave energy extraction device”, Journal of Renewable Energy, 55, 2013, pp 104-119

[3] Cadwell, S.M., Merril, R.A., Sloman, C.M. and Yost, F.L., “Dynamic fatigue life of rubber”, Industrial and Engineering Chemistry, Analytical Edition, Vol 12, No.1, 1940, pp 19-23

[4] Natural Rubber Engineering Data Sheet, Published by the Malaysian Rubber Producers’ Research Association, Tun Abdul Razak Laboratory, 1979

[5] BS ISO 37:2005 Rubber, vulcanized or thermoplastic-Determination of tensile stress-strain properties, pp 1-25

[6] Ahmadi, H.R. and Muhr, A.H., “Modelling dynamic properties of filled rubber”, Plastics, Rubber and Composites Processing and Applications, Vol.26, No.10, 1997, pp 451-461

[7] Bueche, F., “Mullins effect and rubber-filler interaction”, Journal of Rubber Chemistry and Technology, 35, 1962, pp 259-273

[8] Kingston, J.G.R. and Muhr, A.H., “Determination of effective flaw size for fatigue life prediction”, to be submitted to the Journal of Polymer Rubber Chemistry, 2013

[9] Lindley, P.B., Fuller, K.N.G. and Muhr, A.H., NR Technical Bulletin – Engineering design with natural rubber, 1994, pp 1-33